Scientific African 15 (2022) e01043

Contents lists available at ScienceDirect

Scientific African

journal homepage: www.elsevier.com/locate/sciaf

Urban flood susceptibility modelling using AHP and GIS approach: case of the Mfoundi watershed at Yaoundé in the South-Cameroon plateau

Daouda Nsangou[a], Amidou Kpoumié[b], Zakari Mfonka[c], Abdou Nasser Ngouh[a,d], Donald Hermann Fossi[a,e], Camille Jourdan[f], Henri Zobo Mbele[a], Oumar Farikou Mouncherou[e], Jean-Pierre Vandervaere[g], Jules Remy Ndam Ngoupayou[a,*]

[a] Department of Earth Sciences, Faculty of Science, University of Yaounde I, PO Box: 812, Yaoundé, Cameroon
[b] Department of Earth Sciences, Faculty of Science, University of Maroua, PO Box: 814, Maroua, Cameroon
[c] Department of Earth Sciences, Faculty of Science, University of Douala, PO Box: 24157, Douala, Cameroon
[d] National Institute of Cartography (NIC), Laboratory of Image Treatment for Stereo-restitution, P.O. Box:157, Yaoundé, Cameroon
[e] Institute of Mining and Geological Research (IRGM), Hydrological Research Center, P.O. Box: 4110, Yaoundé, Cameroon
[f] Laboratory for the Study of Soil-Agrosystem Interactions-Hydrosystem (LISAH), University of Montpellier, PO Box: 34060, Montpellier cedex 1, France
[g] Institut des Géosciences de l'Environnement (IGE), Université Grenoble Alpes, BP: CS 40700, 38058 Grenoble cedex 9, France

ARTICLE INFO

Article history:
Received 28 May 2021
Revised 28 October 2021
Accepted 2 November 2021

Editor: DR B Gyampoh

Keyswords:
Yaoundé-Cameroon
Multi-criteria decision analysis
Mapping
Flood hazard
Validation

ABSTRACT

Floods are considered as the natural hazards that affect the world's major metropolises the most. Thus, the present study aimed at evaluating the sensitivity to flood risks of the Mfoundi watershed (96.5 km^2) located in the heart of the Cameroonian political capital in a tropical humid forest zone, more precisely in the South Cameroon plateau. The methodological approach adopted was to identify the factors that most favor the risk of flooding in the area from intense literature review and field investigations; the analysis of these factors and the calculation of the Flood Harzard Index (FHI) using the Analytical Hierarchy Process (AHP) approach coupled with the Geographical Information System (GIS) environment. The results reveal that among the ten parameters of the natural environment (elevation, drainage density, rainfall, slope, distance from the river, topographic humidity, hydraulic conductivity, groundwater level, geology and land cover) selected, the land cover, elevation and the geology are the factors that most influences the flooding phenomenon in the area. The value of Flood Hazard Index (FHI) varied from 4.16 to 9.16, the higher the value, the more sensitive the area is to the risk of flooding. Five main classes of flood susceptibility are highlighted: very low, low, moderate, high and very high, representing 9.50, 26, 23, 22 and 19.5%, respectively of the study area. To validate the efficiency of the obtained flood susceptibility map, the adopted Area Under the Curve (AUC) method shows a very good accuracy (0.84 or 84%). The results of this study constitute a basic tool for

* Corresponding authors at: Department of Earth Sciences, Faculty of Science, University of Yaoundé I, PO Box: 812, Yaoundé, Cameroon.
E-mail addresses: nsangoudaoud@yahoo.fr (D. Nsangou), amidou27@yahoo.fr (A. Kpoumié), zakarimfonka@yahoo.fr (Z. Mfonka), n.abdounasser@yahoo.fr (A.N. Ngouh), fdonaldhermann@yahoo.fr (D.H. Fossi), camille.jourdan@umontpellier.fr (C. Jourdan), zmhenri@gmail.com (H.Z. Mbele), omouncherou@yahoo.fr (O.F. Mouncherou), jean-pierrevandervaere@univ-grenoble-alpes.fr (J.-P. Vandervaere), jrndam@gmail.com (J.R. Ndam Ngoupayou).

https://doi.org/10.1016/j.sciaf.2021.e01043

decision-making for environmental management by public authorities and decentralised territorial authorities with territorial jurisdiction.

Introduction

The management of water resources and associated hydrological risks is becoming a major concern in our societies [1]. Being the wide range of hydrological hazards around the world, floods are the most frequent and damaging [2]. Between 1994 and 2013, floods accounted for 43% of recorded natural disasters, affecting nearly 2.5 billion people [3]. During these two decades, floods has caused the death of nearly 158,000 people worldwide and affected more than 2.3 billion people at different levels. While deaths due to floods have declined significantly since the early 1980s, economic losses from flood-related disasters are increasing [4]; they average more than US$23 billion per year [4]. Numerous studies show that population growth, urbanization and climate change will lead to a significant increase in flooding in the coming years [5,6]. These are amplified by the orohydrographic characteristics of the various catchments affected by these extreme phenomena [7].

Cameroon, like other sub-Saharan African countries, is currently facing several hydroclimatological risks and/or disasters (floods, mass movements, violent winds and drought) [6]. These phenomena variably leave human, economic and environmental damage at the heart of many concerns. Between 2007 and 2015, floods affected nearly 367,276 people, leaving them the most risky in the country [8]. In Cameroon, floods are more common to varying degrees in Sudano-Sahelian, humid tropical, continental and coastal cities [9,10]. For example the flood of the 5th September 2020 in Kousseri (Far North Region) which affected more than 10,000 people, almost 400 households and destroyed 150 houses. Those, that occurred on the 18th and 19th November 2016 in Batouri (southern plateau of Cameroon) causing material damage. That of the night of 21st August 2020 in Douala (Littoral Region), which affected around 500 families and left significant material and economic damage. But also the one that occurred very recently in the Douala town on the morning of 12th August 2021, having caused human deaths and destroyed infrastructure (bridges, houses, etc.).

The Yaoundé town (Cameroon's political capital), which is drained by the Mfoundi and Mefou rivers, has witnessed population increase from about 60,000 inhabitants in 1960 [11] to over 3 million in 2017 [12]. This strong demographic growth, combined with anarchic urbanisation, orohydrographic characteristics and highly irregular hydrological regimes, is believed to be one of the factors behind the major runoffs and violent flash floods generated by these topographical subbasins [7,8]. The latter are undoubtedly complementary sources and catalysts for floods, which have often caused significant damage and sometimes loss of human life. Between 1980 and 2016, there was an estimated 171 major floods that caused more than 70 deaths in the country [13]. Surveys of the inhabitants revealed that flood problems appeared from the mid-70s onwards. At the very beginning, there were an average of three floods per year. Since the 1990s, almost every rainy event has led to flooding. For example, the floods of 11th, 12th and 13th October 2019; the floods of 21 May 2020 and the flood of 17th August 2021 which affected several localities in the Yaoundé such as the Central Post Office, the Mfoundi Market, Nsimeyong, Melen, Nkolbissson, Tropicana and Obili.

Indeed, most of the studies related to flooding till date has focused on risks and disasters caused by floods in the Yaoundé town, on the hydroclimatological and hydrological functioning of the Mefou and Mfoundi catchment areas [14,15]; on the hydrological modelling of the Mefou basin [7]; and a summary of inventory of flood zones based on GIS [13]. These studies reveal that rainfall in the zone is abundant and spreads over four seasons unevenly distributed over the year (two rainy seasons and two dry seasons). The observed flows follow variations in the rainfall regime. However, the Mfoundi watershed which drains the Yaoundé town responds more quickly to the intensity and duration of the rains. This is the origin of the resurgence of floods during periods of high rainfall. To address this problem, the government initiated the Yaoundé Sanitation Projects (PADY) for its phases 1 and 2 [7], which led to the construction of a 6.4 km canal on the course of the Mfoundi on 4 of its tributaries, and the implementation of campaigns to clean up certain drains in the city. Despite all these measures taken, floods are becoming more frequent and continue to take a toll [13]. In order to facilitate the implementation of a flood mitigation strategy in the territory, the delineation of flood susceptibility areas based on geo-environmental and anthropogenic factors remains a very effective tool to prevent future damages. This susceptibility to flooding can be further defined as the sensibility or ease with which each area of the basin is flooded [16,17,18,19]. In this regard, several tools and techniques have been developed in recent years. Examples include: 1) the use of field surveys [19,20]; 2) modelling from hydraulic models [21] and mathematical models; 3) the Analytical Hierarchy Process (AHP) [17,18,21,22]; 4) Geographic Information Systems [23]; 5) the use of Geographic Information System (GIS) and different forms of remote sensing (frequency ratio, optical, passive microwave and active microwave) [1,2]; 6) the use of coupled AHP and GIS approaches [16,19]. Among these different techniques and methods, the Analytical Hierarchy Process (AHP) which is a method of multi-criteria decision analysis (MCDA) coupled with GIS is the most widely used. It can take into account a large number of parameters in order

to obtain precise results that are close to reality. This method has already been used in other climatic and morphological environments; but also at the largest scales. However, its application in a medium-sized basin located in the humid tropical forest zone characterized by a rather uneven morphology, a strong urbanization, the notorious incivism of the populations in the environmental management and the impacts of the climate variabilities and/or changes like Mfoundi becomes a necessity.

The Mfoundi watershed, which drains the entire of Yaoundé town, is a victim of flooding every year during the rainy seasons (spring and autumn) [7,13]. Thus, the objective of the present study is to conduct an accurate mapping of flood susceptibilty areas in the urbanized Mfoundi watershed using the Analytical Hierarchy Process (AHP) coupled with the Geographic Information System (GIS). The AHP is established using existing conditions as a reference and previous work [16,17,18,19,22] to evaluate the importance of parameters on defining flood zones. GIS facilitates the processing and analysis of spatial data and facilitates the visualization, interpretation and evaluation of the results of the AHP [16,18]. The approach proposed in this study is applied for the first time in the study area. It allows us to compare the parameters, test them and rank them according to their intervention in the production of flooding in the study area. This technique has already been successfully applied in various fields, including groundwater assessment [23,24] and risk areas (flood, landslide...) [16,25].

Material and methods

Study area

Geographical sitting, climate and oro-hydrography

The Mfoundi watershed is located in Central Africa, precisely in the Center region of Cameroon. It covers an area of 95.6 km^2 entirely urbanised. It extends between latitudes 3° 47′ and 3° 54′ North, and longitudes 11° 29′ and 11° 32′ East (Fig. 1).

The climate of the Mfoundi basin is that of the city of Yaoundé and its surroundings. It is of the transitional tropical and equatorial type with four unevenly distributed seasons (two rainy and two dry seasons) [14,26]: a short rainy season from March to June corresponding to spring; a short dry season (July) corresponding to summer; a long rainy season (August to November) corresponding to autumn and; a long dry season (December to February) corresponding to winter (Fig. 2). The average rainfall and interannual mean temperature are 1,554±261 mm and 24°C, respectively for the period between 1964 and 2019. The dominant vegetation observed in the zone consists of secondary forest that has been severely degraded by human activities.

Geomorphologically speaking, the Mfoundi watershed belongs to the southern Cameroonian plateau with altitudes varying between 670 m and 900 m. The relief is highly rugged, dominated by hills and incelbergs, cut in the shape of half oranges and with convex slopes interspersed with wide marshy valleys that are increasingly inhabited by the expanding population growth. The Mfoundi watershed is a sub-basin of the Mefou (840 km^2) and the latter is a sub-basin of the Nyong (27,800 km^2) which is part of the coastal river basins of Cameroon. The Nyong basin is the second most important river in Cameroon [26] after the Sanaga. The Mfoundi watershed has a dendritic hydrographic network, partially draining 6 of the 7 sub-divisions of the Yaoundé town; the latter Mfoundi takes its source NNW of the city of Yaoundé, at the top of Mount Fébé at an altitude of about 950m. It flows in a N-S direction to join Mefou River at the level of Afan-Oyoa. The main tributaries on the left bank are: the Tongwala, Ntem, Ebogo, Ewoué, Aké, Nkié, Odza rivers; and those on the right bank are: the Abiergueu, Ekozoa and Djoungolo, Mingoa, Olezoa, and Biyemé, Ntsomo and Ezala rivers (Fig. 1 and Table 1). The water transfer from the Mfoundi to the Mefou and to Nyong shows that for an interannual rainfall of between 1,560 mm and 1,750 mm, respective flow coefficients of 80 % are recorded for a Specific Flow (SF) of 42.5 l/s/km^2, 37 % (SF = 20 l/s/km^2) and 18 % (SF = 10 l/s/km^2) [15]. The 2006-2007 flood hydrograph for the Mfoundi River (Fig. A.1) shows several successive peaks in May 2007 (the flood of May 11 with a flow of 12.6 m^3/s, May 21 with 12.6 m^3/s, May 23 with 18, 5 m^3/s, and the 29th with 18.4 m^3/s) which combined with other factors (domestic discharges, state of saturation of the soil, type of rainfall…) were at the origin of the floods of May 29th of this year [27].

Geology and Hydrogeology

The Mfoundi catchment is located in the southern part of the Pan-African Central African mobile chain, which is a collection of Precambrian terrain [28]. It belongs to the Yaoundé Group and consists of metamorphic rocks made up of garnet and biotite gneiss and migmatitic rocks. Three main soil types develop on these basement formations: red ferralitic soils, yellow ferralitic soils and hydromorphic soils [29].

From a hydrogeological point of view, the zone presents two types of superimposed aquifer. A more or less continuous upper porous aquifer hosted in altered rocks and a lower fractured and/or fractured discontinuous aquifer in metamorphic basement formations [30]. Fluctuations in piezometric levels generally follow the rainfall regimes. However, the fluctuations in piezometric levels are much greater at the top of the slopes compared to the lowlands [30].

Description of method

The methodological approach used in this study consisted of: 1) identifying the parameters that have more or less an impact on the flood phenomenon. This was done on the basis of an intense literature review on the flood theme coupled with several field observation campaigns; 2) the calculation of the Flood Hazard Index (FHI) using Analytical Hierarchy

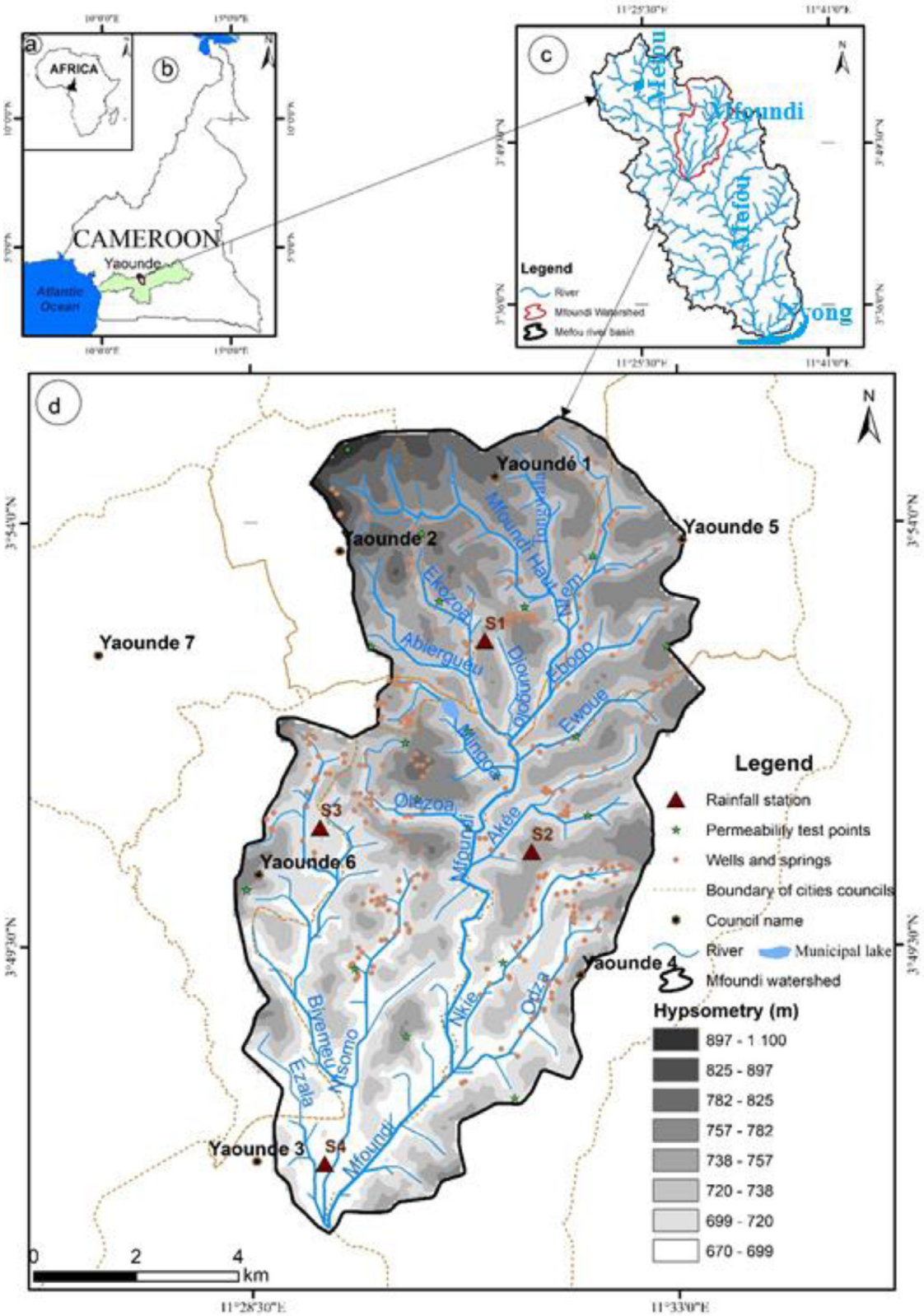

Fig. 1. Location of the study area: **(a)** Cameroon in Central Africa; **(b)** Nyong and Mefou basins in Cameroon; **(c)** the Mfoundi watershed in the Mefou basin; **(d)** the Mfoundi watershed

Table 1
Physiographic characteristics of Mfoundi's elementary catchment areas

Characteristics													
Elementary catchment		X	Y	A(km^2)	P(km)	GC	Form of the basin	Lb(km)	lb(km)	Z. Min(m)	Z. Max (m)	Z. Median (m)	U
Left-bank tributary	**Tongwala**	3° 53′ and 3° 55′	11° 31' and 11° 32'	3.42	9.2	1.4	Rectangle	3.52	0.97	715	770	739	2
	Ntem	3° 52′ and 3° 55′	11° 31' and 11° 33'	5.8	15.0	1.8	Rectangle	6.92	0.83	713	777	745	3
	Ebogo	3°52′ and 3° 53′	11° 32' and 11° 33'	3.38	10.0	1.6	Rectangle	3.07	1.1	700	757	724	2
	Ewoué	3°51′ and 3° 52′	11° 31' and 11° 34'	3.64	10.0	1.5	Rectangle	4.25	0.85	687	770	741	2
	Akée	3°50′ and 3° 51′	11°31' and 11° 33'	4.92	9.2	1.2	Rectangle	3.23	1.52	762	713	736	2
	Nkié	3° 48′ and 3° 50′	11° 31' and 11°32'	5.17	14	1.8	Rectangle	6.16	0.84	660	760	720	2
	Odza	3° 46′ and 3° 50′	11°30′ and 11°32'	6.1	14	1.59	Rectangle	5.96	1.2	670	750	712	2
Right bank tributary	**Abiergueu**	3° 52′ and 3° 54′	11°29′ and 11° 31′	6.25	15.0	1.5	Rectangle	5.58	1.12	715	840	732	2
	Ekozoa	3° 52′ and 3° 54′	11°30′ and 11° 31′	4.03	7.5	1.15	Rectangle	2.53	1.59	712	830	738	2
	Djoungolo	3° 51′ and 3° 53′	11°30′ and 11° 32′	1.42	5.6	1.3	Rectangle	2.08	0.68	705	745	728	2
	Mingoa	3° 51′ and 3° 53′	11°28′ and 11° 31′	3.49	9.0	1.4	Rectangle	3.74	0.93	725	780	760	2
	Olézoa	3° 50′ and 3° 51′	11° 29′ and 11° 31′	3.62	8.44	1.21	Rectangle	3.10	1.12	700	795	740	2
	Ntsomo	3° 48′ and 3° 51′	11°29′ and 11° 30′	8.02	15	1.5	Rectangle	6.32	1.26	680	740	738	2
	Biyéme	3° 46′ and 3° 51′	11°28′ and 11° 30′	12.15	19.0	1.6	Rectangle	8.54	1.42	680	753	719	3

Legend: X=Latitude; Y=Longitude; A= Basin area; P=Perimeter; GC= Gravelius compactness coefficient; Lb= basin length; lb= basin width; Z=elevation; Z. Max=maximum height of the basin; Z. Min=minimum height of the basin; Z. Median=medium height of the basin; U= Stream order.

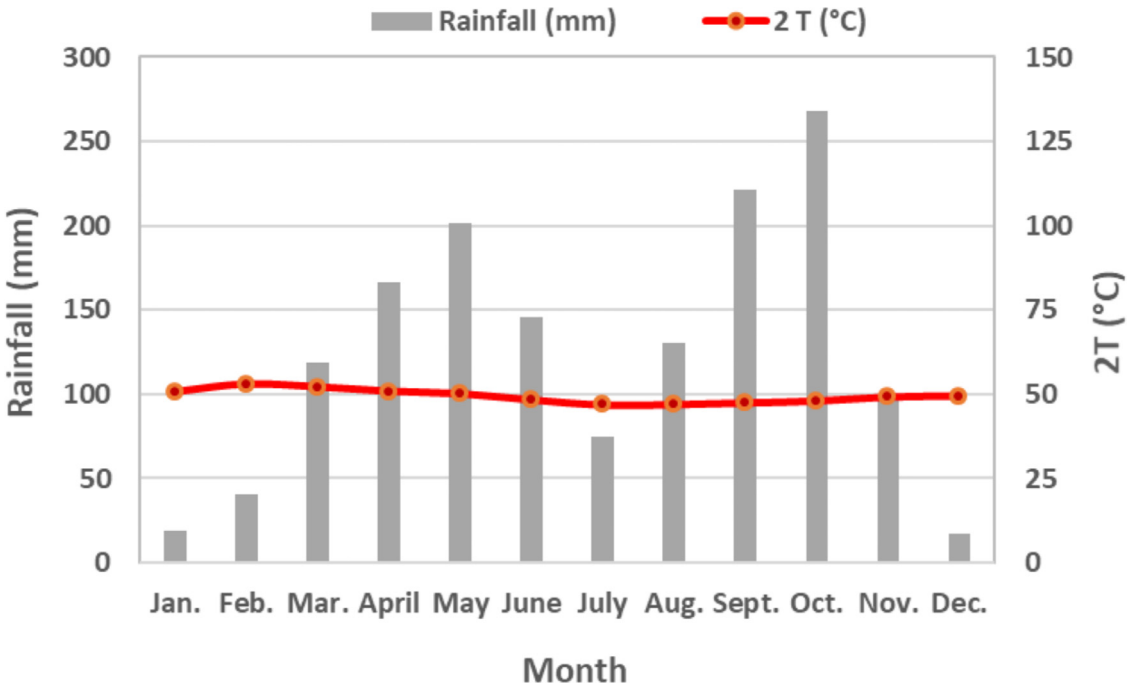

Fig. 2. Ombrothermal diagram of the Yaoundé city, based on the mean monthly variations of rainfall and air temperatures for the period from 1964 to 2019

Process (AHP) and the Geographical Information System (GIS) environment, in order to generate a flood susceptibility map. This methodology was completed by the validation of the latter from the Area Under the Curve (AUC) method based on the verification of field data (different flooding events having taken place in the study area) (Fig. 3).

Identification of the parameters that favour flooding in the area

From the field observations coupled with an intense bibliographical study, 10 parameters have been identified in the Mfoundi catchment area as factors favouring flooding phenomena. On one hand, these are called natural or geo-environmental factors such as: elevation, drainage density, rainfall, slope, distance from the river, topographical humidity, hydraulic conductivity (soil permeability), groundwater level, the presence of swampy areas and geology; and on the other hand, anthropogenic factors consisting of the Land Cover (LC) controlled by galloping population growth and the failure of sanitation systems.

Data sources, mapping and reclassification of parameters

In order to achieve the objective of this work, two types of data were used (Table A.1): i) data collected in the field, which could be called primary data; these are made up of cartographic documents, rainfall records, hydrodynamic characteristics of the aquifer (hydraulic conductivity and groundwater table) and GPS coordinates of the points of occurrence of flooding; ii) secondary data made up of satellite images (Landsat 8 OLI and SRTM). Some data obtained from specialized institutions or by downloading online.

These data were used to map the following parameters:

The land cover map

It was produced from the Landsat 8 OLI (Operational Land Image) sensor satellite image acquired on January 26th 2020. The main stages in the production of this map are: image pre-processing by geometric, radiometric and atmospheric corrections; image enhancement by spectral refinement and noise suppression; image transformation using Principal Component Analysis (PCA); and finally, supervised classification of the image using the maximum likelihood method [31]. The information provided by this map was compared with field observations. Thus, a correction was made using the 3×3 median filter to eliminate isolated pixels and soften the contours of the different classes obtained [2].

Elevation and slope maps

They result from the DEM (Digital Elevation Model) extracted from the global SRTM (Shuttle Radar Topography Mission) image with an accuracy of 30×30 m.

Geological map

The geological map was obtained from the Douala East sheet extracted from the database of the National Institute of Cartography in Yaoundé Cameroon and then digitised.

Rainfall and hydraulic conductivity/permeability maps

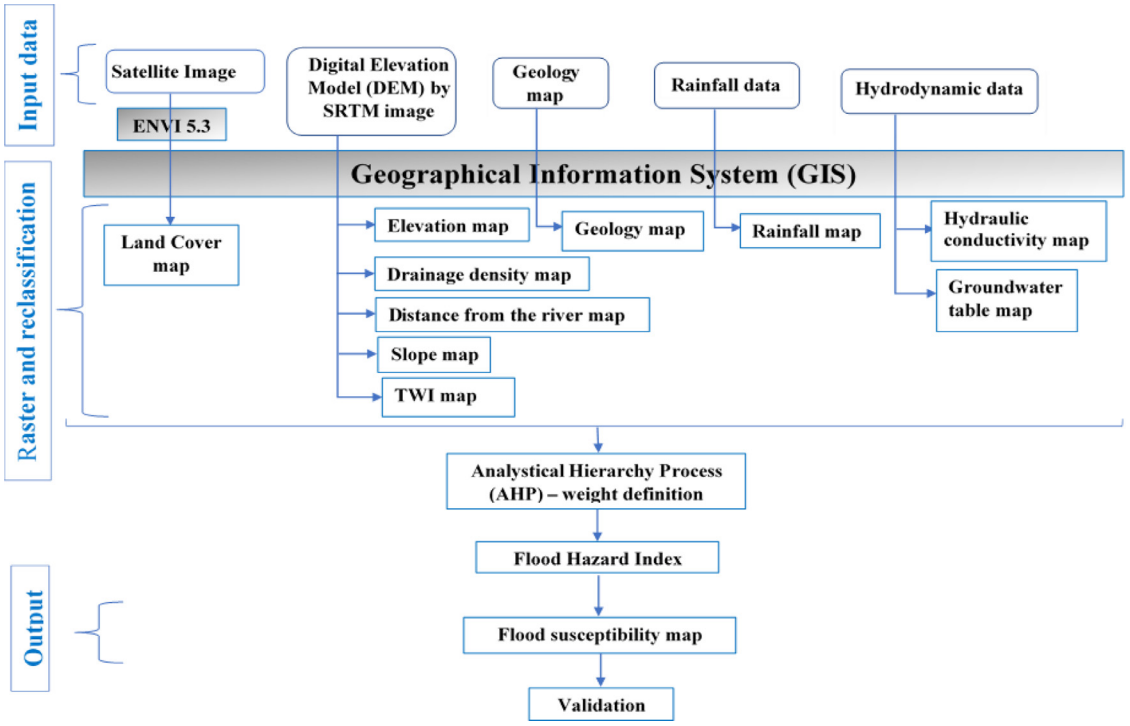

Fig. 3. Conceptual flood susceptibility mapping model based on the analytical prioritization process (AHP) coupled with GIS

They were drawn respectively from monthly average rainfall data obtained from 4 rainfall stations in the study area (Fig. 1); infiltration data, were obtained from permeability tests carried out in the area using Porchet's [32] method; the latter method is extensively described in the literature [33]. The permeability tests were carried out at several points homogeneously distributed over the site. These data were then interpolated using Inverse Distance Weighting (IDW).

The distance from the river map

The distance from the river map derives directly from the map of the river system in the basin, while **the groundwater table** was based on water levels in 267 wells, 59 springs and rivers. The interpolation method used for the latter is spherical kriging.

The drainage density map

It was created using the line density analysis Tool.

The TWI map

The TWI map has been constructed from DEM by running following equation on Raster Calculator [1].

$$\mathrm{TWI} = [\mathrm{Ln}(\mathrm{FLOWACC} \times 900/\tan(\beta))] \quad (1)$$

where FLOWACC is the flow accumulation derived from DEM in the ArcGIS environment and β is the slope (in °).

The ENVI 5.3 and ArcGIS 10.3.1 software was used for processing the LANDSAT 8 OLI satellite image and for producing all the thematic maps, respectively.

The various thematic maps were then subdivided into classrooms. The evaluation of these classes enabled them to be rated according to their degree of influence on flood susceptibility. In order to estimate the ratings of the different parameters in a homogeneous manner, a value scale was developed based on the work of Shaban et al. [34], Ozkan and Tarhan [25] and Hammami et al. [16], also taking into account local environmental conditions. This scale of ratings ranging from 1 (very low) to 10 (very high) (Table A.2). The discretization of the parameters according to this scale helps to obtain the ratings for each class.

Assessment the effect of factors taken in pairs on flood susceptible zone

In order to assess the influence of each factor on flood susceptibility, the factors were correlated two by two. For this purpose, the schematic sketch of Shaban et al. [34] was used. As a general rule, one (1) point is assigned to a factor when it is dominant (major) and 0.5 point when it is minor [16,35]. The sum of points obtained is used to rank the parameters according to their importance on flood susceptibility. This classification is then used for the analytical hierarchy process (AHP) of Saaty [36].

Analytical Hierarchy Process (AHP)

Saaty's AHP [36] allows objective determination of weights or weighting coefficients by comparing factors taken two by two using a matrix. Thus, the first step is to define the decision problem. The second step is to judge the relative importance of the factors based on the Saaty [36] scale (Table A.3) and the development of the comparison matrix. It also makes it possible to determine the weighting coefficient from the eigenvectors of these factors. Each factor was assigned a numerical value between 1 and 9, depending on its importance [25]. A numerical value of 1 means that the two factors being compared are of equal importance. However, a numerical value of 9 means that the factor in the row is much more important than the factor in the column (Table A.3).

Once the matrix has been produced, the third step is the normalisation of the eigenvector values [36]. Finally, the last stage consists in verifying the logic in the judgements through the establishment of properties [22,37]. The latter helped to mathematically synthesise the judgements in order to verify their consistency, based on the calculation of the consistency ratio (CR) [24].

CR is the ratio of IC and RI of a matrix of the same size. This ratio is given by Eq. (2) below

$$CR = \frac{\mathrm{CI}}{RI} \tag{2}$$

where: CI is Consistency Index and RI is Random inconsistency Index;

If CR $\leq$ 0.1 or CR $\leq$ 10%, the matrix is considered to be sufficiently consistent, in case this value exceeds 10%, the assessments may require some revisions.

IC is the ratio between the difference in the value of the consistency vector λmax and the number (n) of factors on the latter minus one. Its mathematical expression is also given by the following Eq. (3):

$$CI = \frac{\lambda\,\mathrm{max} - n}{(\mathrm{n}-1)} \tag{3}$$

The different RI values are shown in table A.4.

Flood susceptibility mapping

The database used for the mapping of areas susceptible to flood risks has been previously processed in the ArcGis software. Each parametric map is elaborated in raster format with a size of 30 $\times$ 30 m. From the dimensions assigned to each parameter class, the "Reclassify" module was used to produce the layers [37]. The aggregation of the different layers using the "Mapcalculator" module made it possible to draw up the final flood risk susceptibility map of the Mfoundi catchment area. The iterative calculation of the Flood Risk Index (FHI) was carried out according to Eq. (4) and (5) below:

$$FHI = \sum_{i=1}^{n} W_i F_i \tag{4}$$

Where: ***Wi*** correspond to the weight of each factor;

Fi the rating of the factor and ***n*** the number of parameters;

This Eq. (4) can also be written in a more developed form presented by the following Eq. (5):

$$\mathrm{FHI} = W_{\mathrm{LULC}}F_{\mathrm{LULC}} + W_{\mathrm{EL}}F_{\mathrm{EL}} + W_{\mathrm{LT}}F_{\mathrm{LT}} + W_{\mathrm{RF}}F_{\mathrm{RF}} + W_{\mathrm{DD}}F_{\mathrm{DD}} + W_{\mathrm{DE}}F_{\mathrm{DE}} + W_{\mathrm{SL}}F_{\mathrm{SL}} + W_{\mathrm{PE}}F_{\mathrm{PE}} + W_{\mathrm{TWI}}F_{\mathrm{TWI}} + W_{\mathrm{GL}}F_{\mathrm{GL}} \tag{5}$$

Where W_{LULC}, F_{LULC}, W_{EL}, F_{EL}, ... represent the weight and rating of the LULC and elevation respectively.

Validation

The Area Under the Curve (AUC) method was used to validate the flood susceptibility map of the Mfoundi watershed. This simple method, based on the verification of past occurrences and scientifically justified, allows the accuracy of the AHP model to be verified. It has already been used in several studies and is considered the most appropriate method to validate AHP models [6,17,18]. For the present study, the AHP-based flood susceptibility map (FHI) was subdivided into 100 classes and the number of pixels belonging to each class was determined. The flood occurrence points were then overlaid on the resulting map, and the number of flood occurrences for each class was listed. Based on this, the cumulative area of the different classes (plotted on the "X" axis) and the cumulative number of flood occurrences (plotted on the "Y" axis) were calculated on a normalized scale from 0 to 1. Then, we calculated the Area Under the Curve (AUC) using the Eq. (6) [18]:

$$\mathrm{AUC} = \sum_{i=1}^{n=100} \frac{(X_1 + X_2)}{2(Y_2 + Y_1)} \tag{6}$$

Where:

X denotes the cumulative percentage of the area (highest to lowest);

Y denotes the cumulative percentage of flood occurrences;

1 and 2 are two sequential classes of data and n is the number of classes (for our study, n = 100).

The AUC value ranges from 0.00 to 1.00, where 0.50-0.60 indicates low accuracy; 0.61-0.70 indicates moderate accuracy; 0.71-0.80 indicates good accuracy; 0.81-0.90 indicates very good accuracy; and 0.91-1.00 indicates excellent accuracy [38].

Table 2
Classes of factors according to different weights

N°	Factors	Class	Descriptive level	Rating	Factor weight	Class weight	ClassWeight (%)
1	**Land cover**	Built	Very high	10	0.2	2	38
		Swampy area	High	8		1.6	31
		Agricultural/bare soil	Medium	5		1	19
		Green area	Low	2		0.4	8
		Forest	Very low	1		0.2	4
2	**Elevation (m)**	670–700	Very high	10	0.17	1.7	38
		700–730	High	8		1.36	31
		730–760	Medium	5		0.85	19
		760–840	Low	2		0.34	8
		> 840	Very low	1		0.17	4
3	**Geology**	Migmatite and garnet biotite gneiss	Very high	10	0.17	1.7	100
4	**Rainfall (mm)**	1,599–1,653	Very Low	1	0.13	0.13	4
		1,653–1,707	Low	2		0.26	8
		1,707–1,761	Medium	5		0.65	19
		1,761–1,815	High	8		1.04	31
		1,815–1,870	Very High	10		1.3	38
5	**Drainage density (km/km²)**	0.12–0.75	Very Low	1	0.11	0.11	4
		0.75–1.15	Low	2		0.22	8
		1.15–1.50	Medium	5		0.55	19
		1.5–1.85	High	8		0.88	31
		1.85–2.61	Very High	10		1.1	38
6	**Distance from the river (m)**	0–102	Very high	10	0.07	0.7	38
		102–210	High	8		0.56	31
		210–310	Medium	5		0.35	19
		310–431	Low	2		0.14	8
		431–815	Very low	1		0.07	4
7	**Slope (%)**	0–2	Very high	10	0.06	0.6	38
		2–5	High	8		0.48	31
		5–10	Medium	5		0..3	19
		10–25	Low	2		0.12	8
		>25	Very low	1		0.06	4
8	**Hydraulic conductivity (m/s)**	$1.4*10^{-8}$–$9.2*10^{-6}$	Very high	10	0.04	0.4	42
		$9.2*10^{-6}$–$2.6*10^{-4}$	High	8		0.32	33
		$2.6*10^{-4}$–$4.5*10^{-4}$	Medium	5		0.20	21
		$4.5*10^{-4}$–$8.3*10^{-4}$	Low	2		0.08	4
9	**Topographical wetness index (TWI)**	5–7	Very Low	1	0.03	0.03	4
		7–8	Low	2		0.06	8
		8–9	Medium	5		0.15	19
		9–11	High	8		0.24	31
		11–15	Very high	10		0.3	38
10	**Groundwater table (m)**	0–2	Very high	1	0.02	0.02	4
		2–4	high	2		0.04	8
		4–6	Medium	5		0.15	19
		6–8	low	8		0.16	31
		8–23	Very low	10		0.2	38

Results and discussion

Multi-influencing factors of flood-susceptible zone

The ten (10) factors selected for the mapping of the flood susceptibility of the Mfoundi basin intervene at varying degrees and independently. Thus each factor is subdivided into classes to which are assigned ratings whose values are proportional to the degree of influence of the class.

Land cover map

Land cover has a significant influence on flooding [5,6]. While vegetation favours the infiltration process, buildings, uncontrolled land use and other urban development tend to promote runoff, which increases flooding. The land cover map of the Mfoundi catchment area is shown in Fig. A.2a. It is subdivided into five classes: built-up areas, which account for 62% of the area of the basin; swampy areas (8%); agricultural areas and bare land (25%); green areas (3%) and finally forest (2%). Ratings of 10, 8, 5, 2 and 1 have been assigned to each class according to its influence on flooding (Table 2).

Elevation map

Elevation plays a very important and effective role in flood susceptibility [39]. The lower it is, the more likely the area is to be flooded, as low-lying areas are the points of convergence of the various rivers [6]. The Mfoundi watershed is developed on a rugged terrain with altitudes between 670 m and 1100 m for an average of 750 m. The map of elevations in the area shown in Fig. A.2b has been subdivided into five classes (670 - 700 m, 700 - 730 m, 730 - 760 m, 760 - 840 m and > 840 m) represented by the following respective percentages: 22%, 26%, 38%, 12% and 2%. These different classes have been assigned grades 10, 8, 5, 2, and 1, respectively (Table 2).

Geology map

The geology of the area is one of the significant factors used to define flood zones. This factor is closely related to the permeability that varies from one rock to another. The infiltration of rainwater is less important for an impermeable rock, which favors the stagnation of water and the extension of runoff surfaces that will amplify the flood risks [16]. The geological formations encountered in the study area are mainly composed of migmatites and biotite and garnet gneisses (Fig. A.2c). These rocks are all impermeable and correspond to one class that has been assigned a rating of 10 (Table 2). The geological formations encountered in the study area are mainly composed of migmatites and biotite and garnet gneisses (Fig. A.2c). These rocks are all impermeable and correspond to one class that has been assigned a rating of 10 (Table 2).

Rainfall map

Precipitation is the main trigger of flooding [9]. After a rainstorm or a succession of rainstorms, streams can move beyond their beds. However, the amount of rainfall that falls in a locality is not equal at every point in the area [39]. As a result, areas with the greatest rainfall amounts will be considered susceptible to flooding. The rainfall distribution map in the Mfoundi basin is divided into 5 classes ranging from 1,559 mm to 1,870 mm with an amplitude of about 55 mm; these interannual rainfall amounts decrease from west to east (Fig. A.2d). To these five classes are respectively assigned ratings 10, 8, 5, 2, and 1 (Table 2), each rating being proportional to the degree of susceptibility of the parameter to the flooding phenomenon.

Drainage density map

Drainage density is defined as the ratio of the total length of streams in a watershed to the area of the watershed. The higher the drainage density of an area the more likely it is to be flooded which justifies its significant impact on flood occurrence [9]. The drainage density map shown in Fig. A.2e has been reclassified into five classes, with values ranging from 0.12 to 2.61 km/km^2. These values are high around watercourses and at confluences. Based on its significant contribution to the flooding process, the highest density class has been assigned a rating of 10, while the lowest density class has been assigned a rating of 1 (Table 2).

Distance from the river map

The distance from the river is a factor generated from rivers which highlights the flood risk due to proximity to the channel [37]. The distance map of the area has five main classes: 0 - 102 m; 102 - 210 m; 210 - 310 m; 310 - 431 m; 431 - 815 m (Fig. A.2f). The distance from the river class with the lowest values (0 - 102 m) has a high risk of flooding and therefore has a score of 10. Those with high distance from the river values (431 - 815 m) have the opposite effect. The latter class has been assigned a rating of 1 (Table 2).

Slope map

Slopes influence surface runoff and rainwater infiltration [16,18]. Areas with low slopes flood more quickly because of the low surface runoff velocity. Areas with high slopes, on the other hand, have high runoff velocity that is incompatible with flooding [17]. The slope map in the Mfoundi basin expressed in % shows five classes ranging from 0 to 33%. This area is dominated by slopes below 5% (Fig. A.2g). The lowest class with slopes between 0 and 2% has a slope of 10, while the highest class (> 25%) has a slope of 1. It is important to note that the latter class is the least represented in the study area (Table 2).

Hydraulic conductivity map

The hydraulic conductivity of a soil is the capacity of the soil to allow water to pass through it [40]. The latter provides an estimate of how quickly water infiltrates a soil [40]. This infiltration rate varies from soil to soil, permeability values will be low in a clay soil and higher in a sandy soil. The hydraulic conductivity map shows four classes of hydraulic conductivity with values ranging from 9.2×10^{-6} m/s to 8.3×10^{-4} m/s (Fig. A.2h). Thus, the highest rating (10) was assigned to the lowest hydraulic conductivity class (9.2×10^{-6} and 2.6×10^{-4} m/s). This class is more important for the flooding phenomenon, because its low value accentuates the stagnation of water. The lowest rating (2) was assigned to the highest classes (4.5×10^{-4} and 8.3×10^{-4} m/s) (Table 2).

Topographical Wetness Index map

The TWI highlights the relatively flat and naturally wet areas in the catchment [1,17]. The higher this parameter value the more floodable the area [17]. In the present study, the TWI map presented in Fig. A.2i is divided into five classes with values ranging from 5 to 15. The class with a TWI between 11 and 15 is assigned a score of 10. The class with TWI between 5 and 7 has been assigned a rating of 1 (Table 2).

Groundwater table map

Groundwater levels vary between areas. Groundwater rise can be the cause of flooding, this is materialized by the influence of meteoric water (rainfall) that infiltrates at a high speed into the aquifer and can affect the infiltration capacity of the soil. In this way, it increases the hydraulic pressure in the aquifer and in areas where groundwater is very close to the surface [40]. The map of groundwater levels in the area has been divided into five classes (0 - 2 m; 2 - 4 m; 4 - 6 m; 6 - 8 m and 8 - 28 m) (Fig. A.2j). The areas of low static level (0 - 2 m) have a rating of 10 (Table 2); this covers about 20% of the area of the basin. It should be noted that the depth of the water table decreases progressively from the North-West sector to the South-East sector of the study area.

Interrelationship and pairwise comparisons of the factors flood Hazard

As not all factors have the same degree of influence in the flood generation mechanism in the area, it is necessary to determine the weight of each factor in relation to the phenomenon being studied.

Multi-influencing factors of flood susceptible zone

Determining risk areas can only be possible if each factor is taken independently. The relationship of Shaban et al. [34] applied to the factors in order to assess the influence of each of them on flood susceptibility is summarised in Fig. A3. It is shown that: for two parameters separated by a discontinuous arrow, the one towards which the arrow is pointed is dominant in relation to the other; conversely, when the line is continuous between two parameters, the one towards which the arrow is pointed is less dominant, in this case we speak of a minor element. The sum of the numbers of points of each risk factor is recorded in Table A.5. The descending order of all these parameters according to their sensitivity to the phenomenon understudy is as follows: the LC which totals 9 points, followed by the elevation and geology which total the same number of points (8), rainfall (7.5), drainage density (7), Distance from the river (6.5), slope (6), permeability (5.5), TWI (5) and Groundwater table (4.5).

Weights of factors

The matrix comparing pairs of parameters was carried out to determine the weight of each factor (Table A6). On this basis, the first row of this matrix shows the importance of land cover (LC) with respect to other parameters. It is noted that LC is considered more important than groundwater level, and therefore has been assigned the numerical value 8. Calculation of the weighting coefficients (W) from the eigenvectors of the ranking matrix reveals that the minimum value of 0.02 corresponds to the weight of groundwater levels and the maximum value of 0.20 corresponds to the weight of land cover (Table A.6). Thus, the groundwater level is considered to be the least important factor in the flood generation process and the land cover is the most important.

Consistency Ratio

The Consistency ratio is used to check the consistency of judgements. In this study, the RI and Consistency index (CI) values for the ten (10) parameters used are 1.49 and 0.062, respectively, for a consistency ratio of the order 0.05 or 5% (Table A.7). This last value is less than 10%, which proves that the hierarchical matrix is acceptable [36]. This CR value is higher than that obtained by Hammami et al. [16] (0.013 or 1.3%) and lower than those of Kazakis et al. [22] and Ake et al. [24], with values of 0.08 (8%) and 0.07 (7%), respectively, obtained within the framework of the mapping of flood zones on the one hand and that of potential groundwater recharge zones on the other hand. However, these values vary according to the number of parameters used and the shoreline values assigned to each decision parameter.

Classes of the factors according weights

The contribution of the classes of factors used to produce the flood susceptibility map are shown in Table 2. It is the ratio of the weight of each class and the sum of the weights of the classes of the factor under consideration. The results are expressed as a percentage. Thus, for the elevation factor, it can be noted that the area between 670 and 700 m is much more significant compared to the other classes (700 - 730 m, 730 - 760 m, 760 - 780 m and > 840 m). The rainfall factor shows that the high rainfall class (1,815 - 1,870 mm) is much more significant compared to the other classes (1,761 - 1,815 mm, 1,707 - 1,761 mm, 1,653 - 1,707 mm, 1,599 - 1,653 mm). For the land cover factor, the area of the buildings has more influence on the phenomenon compared to the other classes (swampy area, agricultural/soil, green area and forest).

Flood Hazard Index

The Flood Hazard Index (FHI) is related to the values of the factor weights associated with the respective ratings of the different layers [16]. It was calculated in a GIS according to Eq. (7). The Flood Hazard Index (FHI) values obtained vary from 4.16 to 9.16. The higher the value, the more sensitive the area is to flood risk.

$$\mathbf{FHI} = 0.20F_{LULC} + 0.17F_{EL} + 0.17F_{LT} + 0.13F_{RF} + 0.11F_{DD} + 0.07F_{DE} + 0.06F_{SL} + 0.04F_{PE} + 0.03F_{TWI} + 0.02F_{GL} \quad (7)$$

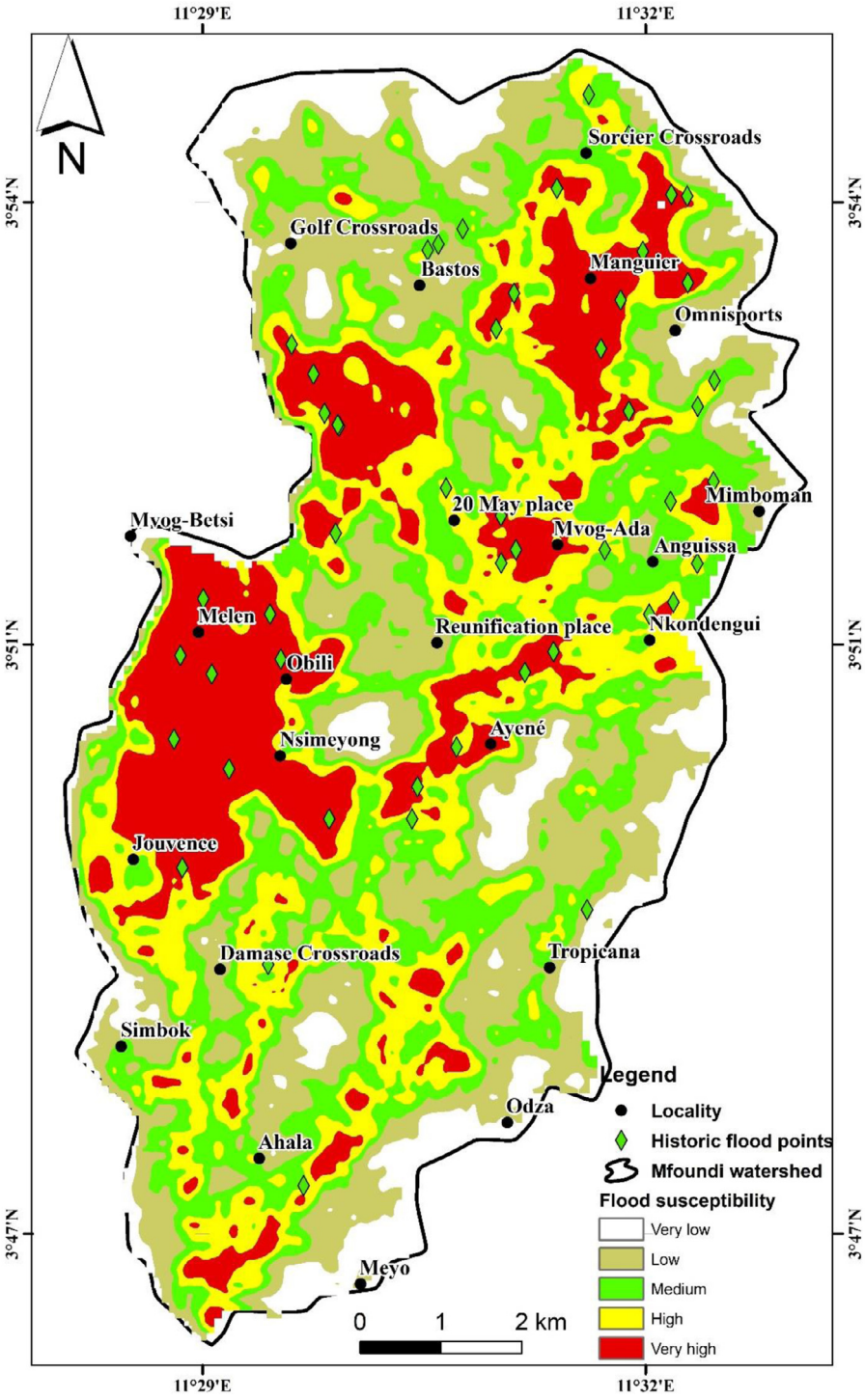

Fig. 4. Flood susceptibility map of the Mfoundi watershed including 50 historic flood points

Flood susceptibility map

The flood susceptibility map obtained by thematic mapping coupled with AHP and then classified based on natural break algorithm in the ArcGIS environment highlights five major classes of flood susceptibility, ranging from very low class to very high class (Fig. 4). These are:

Fig. 5. Some human activities which favor the flood in the Mfoundi watershed: **(a and b)** discharge of urban waste in the river bed; **(c)** embankment; **(d)** swamp occupation

- the very low flood risk class which represents 9.50% of the study area; it is located at the level of the crest lines of the Mfoundi basin and its sub-basins;
- the weak class, which covers 26% of the study area and is scattered throughout the basin;
- the moderate class, which covers 23% of the study area;
- the high class which covers 22% of the study site is more represented in the central part, but slightly scattered in the northern and southern parts and;
- the very high class which spreads over 19.5% of the surface area and is observed everywhere in the study zone, at times seen as isolated islets with extensions to the North.

The tests of Shaban et al. [34] and Saaty [36] applied to the present work reveal that the factors that considerably influence the flood phenomenon are land cover, elevation and geology. These same factors were highlighted by Hammani et al. [16] in the Tunis region where he used 8 weighting factors over an area of about 524.4 km^2 to map flood-prone areas. On the other hand, the work of Kazaski et al. [22] carried out in the Rhodope-Evros region in Greece (5,004 km^2) using seven (7) factors shows that the factors influencing flood susceptibility are, in order of importance, the flow accumulation, distance from drainage network and elevation. Those of Das and Gupta [19] in the Subarnarekha basin (India) applied to 12 factors reveal that the factors that most influence flood susceptibility in this area are elevation, slope, TWI and drainage density. In contrast to the results obtained in the present study, Das and Gupta [19] state that geology is the least influential factor on flooding in the Subarnarekha basin. This difference would be related to the presence of outcrops of impermeable rocks scattered throughout the Mfoundi watershed and more particularly on the hillsides, riverbanks and their beds that promote rapid runoff of floods and stagnation of water with consequent flooding phenomena [16,18].

The superposition of the points regularly subject to flooding to the final map reveals that the majority of these points (94%) are located respectively on the areas of very high susceptibility (18.65 km^2) and high (21.98 km^2) (Table A.8). These areas are generally located in built-up and swampy areas with outcrops of impermeable geological formations and low altitudes and slopes. The regularly flooded points which are located respectively on the zones of weak (23.05 km^2) and moderate susceptibility are not represented (21.98 km^2) (Table A.8). The recurrence of flooding phenomena in these areas can be explained by: the undersizing of sanitation works (canalisation and evacuation of rainwater) (Fig. 5a, 5c); the lack of civic responsibility of the population in the practice of sanitation measures (discharge of solid and liquid waste into the drains) and the failure in the maintenance of hydraulic works (Fig. 5b, 5d). In recent years, the various rivers draining the

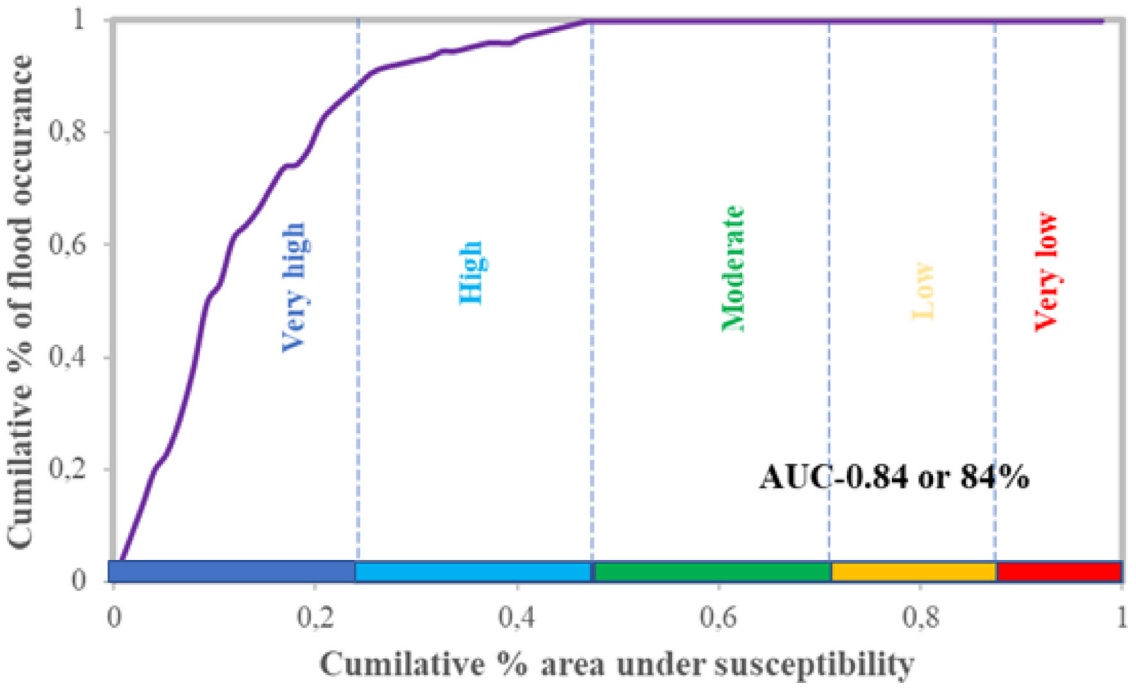

Fig. 6. Area under the curve (AUC) related to susceptibility model validation [[17,18] modified].

Mfoundi catchment area have been filled with plastic bottles of mineral and brewed water, which have still not found a sector for recycling (Fig. 5a, 5b).

The methodology developed in this study can be applied in another area. The only difference is that the evaluation of the parameters that would be included in this flood susceptibility mapping should take into account the local realities and specifics of each environment.

Validation of flood susceptibility map

The validation of the flood susceptibility map generated by the AHP approach coupled with GIS was based on the AUC of past flood occurrence points in the study area (Fig. A.4a, 3b, 3c). The high AUC value (0.84 or 84%) obtained demonstrates a very good accuracy of the flood susceptibility map of the Mfoundi watershed (Fig. 6). This AUC value is similar to those obtained by Das [17,18] respectively for the flood susceptibility mapping of Western Ghat coastal belt (applied to 12 factors) and Ulhas basin (applied to 11 factors) all located in India. On the other hand, the works of Das and Gupta [19] in the Subarnarekha basin (India) and Rahman et al. [6] in the Surma River basin (northeast Bangladesh) all applied to 12 factors reveal AUC values greater than 0.90 (90%) which reflects that the flood susceptibility maps obtained in these studies are excellent. The AUC value obtained in the present study is within the wide range of values obtained in the other study cases. However, the accuracy of the final map obtained in this study accurately verifies the methodology adopted. Therefore, the latter provides a baseline information, which should be taken into account in the urbanization plan, but also in the flood management measures by the decision makers.

Limitations of the methodology and recommendation

Despite some imperfections related to the quality of the medium resolution image (SRTM 30 m) used in the present study, the subjectivity of the coastlines attributed/assigned to certain parameters, the fact remains that the flood susceptibility map of the Mfoundi watershed obtained constitutes a real tool for development, planning and decision-making by the administrative authorities and the decentralized territorial communities with jurisdiction. The results of this work will undoubtedly contribute to the improvement of the living conditions of the populations of this intensely populated area where the problem of environmental management and sanitation constitute a real bottleneck.

Indeed, the map obtained in accordance with the field observations. However, it would be necessary in future work to integrate these impertinences and at best, to try out more efficient models capable of reducing the margins of error to a minimum.

This work is the first of its kind to use a wide range of environmental data (SRTM, rainfall, geology...) to assess the susceptibility of the Mfoundi watershed to flooding in a context of global change. These results constitute a first step in the

search for a solution to the flooding problems in the Yaoundé town; they will also allow the administrative authorities, the government and the decentralized territorial communities and all other development actors to achieve synergy of action in the interventions before, during and after the floods in this city. From a scientific point of view, this work will not only allow us to better understand the environment of the Mfoundi watershed, but also to identify and evaluate the parameters that control the risk of flooding.

Conclusion

The objective of this study was to map the areas of susceptibility to flooding in the Mfoundi catchment area for better environmental management based on ten parameters of the natural environment (elevation, drainage density, rainfall, slope, distance from the river, topographic humidity, hydraulic conductivity, groundwater level, geology and land cover) using the Analytical Hierarchy Process (AHP) and the GIS environment. In terms of results:

- the value of the consistency ratio (0.05 or 5%) indicates that the prioritisation matrix is acceptable; this varies according to the scores assigned to each factor;
- the Flood Hazard Index (FHI) varied from 4.16 to 9.16, the higher the value, the more sensitive the area is to the risk of flooding;
- five main classes of flood susceptibility have been identified: the very low class representing 9.50%, the low class covering 26%, the moderate class (23%), the high class (22%) and the very high class (19.5%);
- the test of Shaban et al. [34] and AHP show that the land cover, elevation and the geology are the main factors which considerably contribute to the flood phenomenon;
- The flood susceptibility map obtained by AHP showed a very good accuracy (AUC: 84%).

Despite some imperfections in the method linked to the subjectivity of the AHP (Analytical Hierarchy Process) in terms of weight estimation, the results obtained constitute a real decision-making aid tool for planning and development by public authorities and decentralised local authorities in a context of local development. Indeed, the map obtained is in conformity with the field observations. However, it would be necessary in future work, to integrate these impertinences and at best, to try out more efficient models capable of reducing the margins of error to a maximum.

Declaration of Competing Interest

The authors declare that they have no known competing financial interests or personal relationships that could have appeared to influence the work reported in this paper.

Acknowledgements

The authors thank the LMI DYCOFAC of the French National Research Institute for Development (IRD) for their support; Department of National Meteorology (DNM) of the Ministry of Transport of Cameroon (MINTRANS) for generously providing weather data, Mr. Willy Franck SOB (SOGEFI-Cameroon) for his collaboration and Dr Mouafo Lucas of the University of Yaoundé I for amending the language.

Funding

This research received no specific grant from any funding agency in the public, commercial, or not-for-profit sectors.

Supplementary materials

Supplementary material associated with this article can be found, in the online version, at doi:10.1016/j.sciaf.2021.e01043.

References

[1] D. Sarkar, P. Mondal, Flood vulnerability mapping using frequency ratio (FR) model: a case study on Kulik river basin, Indo Bangladesh Barind region, Applied Water Science (2020).
[2] R.K. Samanta, G.S. Bhunla, P.K. Shit, H.R. Pourghasemi, Flood susceptibility mapping using geospatial frequency ratio technique: a case study of Subarnarekha River Basin, Model Earth Syst Environ, India (2018).
[3] UNISDR, The human cost of natural disasters 2015: A global perspective, 2015.
[4] UN, World Urbanization Prospects 2018. New York: United Nations Department of Economic and Social Affairs (UN-DESA), Population Division. May (16) Retrieved from United Nations Department of Economic and Social Affairs, 2018.
[5] R. Magdalena, Agnoletti M, A. Alaoui, J.C. Bathurst, G. Bodner, M. Borga, V. Chaplot, et al., Land use change impacts on floods at the catchment scale: Challenges and opportunities for future research, Water Resour (2017) Res. 53.
[6] M. Rahman, C. Ningsheng, G.I. Mahmud, M.M. Islam, H.R. Pourghasemi, H. Ahmad, M.J. Habumugisha, R.M.A. Washakh, M. Alam, E. Liu, Z. Han, H. Ni, T. Shufeng, A. Ashraf Dewan, Flooding and its relationship with land cover change, population growth, and road density, Geoscience Fontiers 12 (2021) 101224.
[7] CRED, Natural disasters in 2018, Lower mortality, higer cost, CRED Crunch, N° 29 (2018) 5–6.
[8] H. Bang, L. Miles, R. Gordon, The irony of flood risks in African Dryland Environments: Human Security in North Cameroun, World Journal of Engineering and Technology (2017) 109–121.

[9] P.S. Kouassy Kalédjé, J.R. Ndam Ngoupayou, A. Fouépé Takounjou, M. Zebsa, J. Mvondo Ondoa, Floods of 18 and 19 November 2016 in Batouri (East Cameroon): Interpretation of the Hydro-Meteorological Parameters and Historical Context of the Post-Event Survey Episode, Hindawi. The Scientific World Journal (2019) Article ID 3814962, 7.
[10] A. Franqueville, Croissance démographique et immigration à Yaoundé, Cah. O.-m. 32 (1979) 321–354.
[11] UNDESA, World Population Prospects: The 2017 Revision, Key Findings and Advance Tables, 2017.
[12] C. Jourdan, in: Approche mixte instrumentation-modélisation hydrologique multi-échelle d'un basin tropical peu jaugé soumis à des changements d'occupation des sols: Cas du bassin de la Méfou (Yaoundé, Cameroun), Thése de Doctorat/Phd Univ. Montpellier., 2019, p. 369.
[13] M.Moffo Zogning, in: Contribution des systèmes d'information géographique pour la cartographie des zones à risques inondables à Yaoundé: application au bassin versant du Mfoundi, Mém de Mast Univ Liège, 2017, p. 255.
[14] D. Sighomnou, Analyse et redéfinition des régimes climatiques et hydrologiques du Cameroun: perspective d'évolution des ressources en eau, Th. Doc. Etat Univ. Ydé. I (2004) 289.
[15] J.R. Ndam Ngoupayou, R. Apouamoun Yiagnigni, S. Youego, P.M. Ngnike, J.L. Boeglin, J.P. Bedimo, Transfert d'eau et de matières dans un écosystème forestier urbanisé en Afrique: le bassin versant de la Méfou au sud du Cameroun, in: D. Orange, E. Roose, P. Vermande, J-P (Eds.), In Actes JSIRAUF (Journée Scientifique Inter Réseau de l'AUF), Gastellu–Etchegorry and pham Quang Ha, 2007, pp. 13–18.
[16] S. Hammami, L. Zouhri, D. Souissi, A. Souei, A. Zghibi, A. Marzougui, M. Dlala, Application of the GIS based multi-criteria decision analysis and analytical hierarchy process (AHP) in the flood susceptibility mapping (Tunisia), Arabian Journal of Geosciences 12 (2019) 653.
[17] S. Das, Geospatial mapping of flood susceptibility and hydro-geomorphic response to the floods in Ulhas basin, India. Remote Sensing Application: Society and Environnement 14 (2019) 60–74.
[18] S. Das, Flood susceptibility mapping of the Western Ghat coastal belt using multi-source geospatial data and analytical hierarchy process (AHP), Remote Sensing Application: Society and Environnement 20 (2020) 100379.
[19] S. Das, A. Gupta, Multi-criteria decision based geospatial mapping of flood susceptibility and temporal hydro-geomorphic changes in the Subarnarekha basin, India. Geoscience Fontiers 12 (2021) 101206.
[20] Y. Sado-Inamura, K. Fukushi, Empirical analysis of flood risk perception using historical data in Tokyo, Land Use Policy 82 (March) (2019) 13–29.
[21] G.L. Cea, C.E. Bladé, R.M. Sanz, I. Fraga, E. Sañudo, O. García-Leal, M. Gómez-Gesteira, J. González-Cao, Benchmarking of the Iber capabilitiesfor 2D free surface flow modelling. A Coruña. Universidade da Coruña, Servizo de Publicacións. ISBN: 978(2020) 84-9749-764-0.
[22] N. Kazakis, I. Kougias, T. Patsialis, Assessment of flood hazard areas at a regional scale using an index-based approach and analytical hierarchy process: application in Rhodope–Evros region, Greece. Sci Total Environ 538 (2015) 555–563.
[23] P.S. Ozkan, C. Tarhan, Detection of flood hazard in urban areas using GIS: Izmir case, Procedia Technology 22 (2016) 373–381.
[24] Oikonomidis D, S. Dimogianni, K. Kazakis, K. Voudouris, A GIS/remote sensing-based methodology for groundwater potentiality assessment in Tirnavos area Greece, Journal of Hydrology 525 (2015) 197–208.
[25] J-C. Olivry, in: Fleuves et rivières du Cameroun, Monographies Hydrologiques, ORSTOM, Paris, 1986, p. 488.
[26] T.D. Nguemou, Hydrologie et transports solides dans un écosystème forestier urbanisé: Exemple du bassin versant du Mfoundi au centre sud du Cameroun, Mém. DEA. Fac des sci. Yaoundé I (2008) 83.
[27] S. Owona, B. Schulz, L. Ratschbacher, J. Mvondo Ondoa, G.E. Ekodeck, M.F. Tchoua, P. Affaton, Pan-African metamorphic evolution in the southern Yaounde Group (Oubanguide Complex, Cameroon) as revealed by EMP-monazite dating and thermobarometry of garnet metapelites, Journal of Afrcan Earth Sciences 59 (2011) 125–139.
[28] P.-D. Ndjigui, M.F.B.B. Badinane, H.P.K.Nandjip Nyeck, P. Bilong, Mineralogical and geochemical features of the coarse saprolite developed on orthogneiss in the south Cameroun, J.Afr. Earth Sci (2013) 25–142.
[29] J.R. Ndam Ngoupayou, A.F. Bon, G. Ewodo Mboudou, A.N. Ngouh, G.E. Ekodeck, Hydrogeological Characteristics of Shallow Hard Rock Aquifers in Yaounde (Cameroon, Central Africa), In Intech Open, the world's leading publisher of Open Access books, 2019, p. 17.
[30] B.Ewane Ewane, Assessing land use and landscape factors as determinants of water quality trends in Nyong River basin, Cameroon, Environ Monit Assess 192 (2020) 507.
[31] M. Porchet, Hydrodynamique des puits, Annuaire du Génie Rural, fasc (1931) 60.
[32] O. Banton, M.L. Bangoy, Hydrogéologie, Multisciences environnementale des eaux souterraines. PUQ/AUPELF éd, Sainte-Foy (1997) 460.
[33] A. Shaban, M. Khawlie, C. Abdallah, Use of remote sensing and GIS to determine recharge potential zones: the case of Occidental Lebanon, Hydrogeol J 14 (4) (2006) 433–443.
[34] A. Shaban, M. Khawlie, R.B. Kheir, C. Abdallah, Assessment of road instability along a typical mountainous road using GIS and aerial photos, Lebanon–eastern Mediterranean, Bull EngGeol Environ. 1 60 (2) (2001) 93–101.
[35] T.L. Saaty, The analytic hierarchy process, McGraw-Hill International, New York, 1980.
[36] I. Elkhrachy, Flash flood hazard mapping using satellite images and GIS tools: a case study of Najran City, Kingdom of Saudi Arabia (KSA), National Authority for Remote Sensing and Space Sciences the Egyptian Journal of Remote Sensing and Space Sciences 18 (2) (2015) 261–278.
[37] G.E. Ake, K.J. Kouame, A.B. Koffi, J.P. Jourda, Cartography of potential recharge areas of the Bonoua aquifer (Southeastern Côte d'Ivoire), Journal of Water Science 31 (2) (2018) 129–144.
[38] E. Yesilnacar, T. Topal, Landslide susceptibility mapping: a comparison of logistic regression and neural networks methods in a medium scale study, Hendek region (Turkey), Eng. Geol. 79 (3–4) (2005) 251–266.
[39] J.K. Poussin, W.W. Botzen, J.C. Aerts, Factors of influence on flood damage mitigation behavior by households, Environ Sci Pol 40 (2014) 69–77.
[40] C. Recep, A. Veysel, Evaluation of hydrological and hydrogeological characteristics affecting the groundwater potential of Harran Basin, Arabian Journal of Geosciences 13 (2020) 186.